(昭和47年5月日本造船学会春季講演会において講演)

A Study on Collision by an Elastic Stem to a Side Structure of Ships

Yoshio Akita*, *Member*
Katsuhide Kitamura**, *Member*

Summary

In order to investigate the share of absorbed energy at the time of collision between a nuclear powered ship and other ships, six collision tests were conducted between the side model simulating Japan's first nuclear powered ship (Mutsu) and elastic stem models simulating conventional ships. Destruction modes of both stem and side structure can be grouped according to the strength ratio of a stem to a side structure. Minorsky's calculation method for estimating the absorbed energy is discussed using the test results. Further, design formula for the collision-protective structures of nuclear powered ships is examined.

1 Introduction

In designing nuclear powered ships, it is necessary to provide protective side structures against collision with the stem of other ships. Particularly the section where the vessel containing the reactor is located should not be damaged. At the time when the first nuclear powered ship (Mutsu) was designed and built in Japan, Minorsky's formulae[1] were used for calculating the absorbed energy in a structure and there was a need to check it experimentally. For this purpose collision tests have been conducted for several side models and stem models, and in analyzing the destruction mechanism of side structures, a calculation formulae have been proposed, which show good agreement with experiments. That study has been summarized in the reference 2. In overseas, some experiments were carried out at Naples University in Italy[3] and at GKSS(Gesellschaft für Kernenergie verwertung in Schiffbau und Schiffahrt m.b.H.) in Germany[4]. However, the formula for calculating the absorbed energy has not yet been established.

In the previous study, absorbed energy at destruction in the side structure was calculated on the assumption that only the side structure of nuclear powered ships will break because the stem of the colliding ship is rigid. However, the stems of actual colliding ships are not rigid, but in fact, are more elastic than the side structure in most of nuclear powered ships. Therefore, in a collision accident, the bed energy at destruction of the colliding ship also exists.

The study is aimed at investigating the conditions of sharing the absorbed energy at destruction among the two on the assumption that not only the side structure of the nuclear powered ship but also the stem of the colliding ship will break concurrently. For this purpose, statical collision tests were conducted between side structures simulating Mutsu and elastic stems simulating conventional ships.

By obtaining the relationship between load and penetration, and calculating the absorbed energy, some discussions about the destruction modes, absorbed energy at destruction and examination of design formula were made.

* The Ship Classification Society of Japan, Dr.
** Ishikawajima-Harima Heavy Industries Co., Ltd., Research Institute

2 Outline of Tests

2.1 Side Model

In referring to the section where the vessel containing the reactor is located in Mutsu, the side model is reduced to a scale of about 1/10 of the design dimensions of it, and the same model was used in collision tests by rigid stems in other series of tests. The dimensions of the side model are shown in Fig. 1.

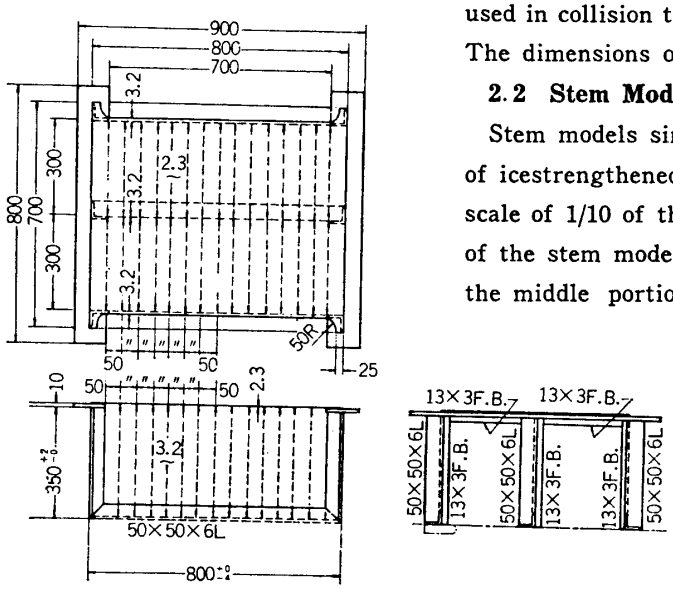

Fig. 1 Side model, Transversely framed structure

2.2 Stem Models

Stem models simulating thoseof conventional ships and of icestrengthened ships or icebreakers, were designed to a scale of 1/10 of the design dimensions. The deck positions of the stem model are set so that they will penetrate into the middle portion of the side shell between decks of the side model. The dimensions of the stem models are shown in Fig. 2. The stem models are of 6 types; T-1 and T-2 of transversely framed type and L-1, L-2, L-3 and L-4 of longitudinally framed type. Comparison between stem models and actual ahips are indicated in Table 1. In this Table Ship A, Ship B and Fuji correspond to an ordinary ship, an ice-strengthened ship, and icebreaker respectively. Stem models T-1 and L-1 correspond to an ordinary ship, T-2, L-2 and L-3 to an ice-strengthened ship, and L-4 to an icebreaker respectively.

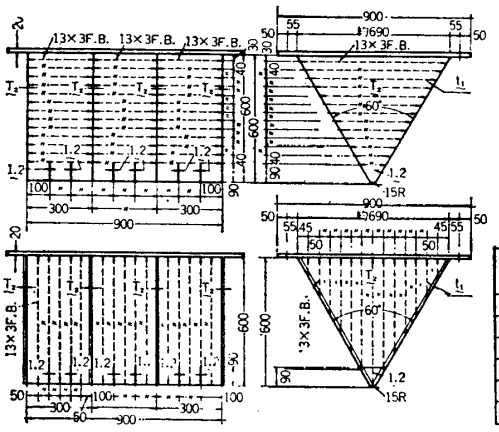

STEM MODELS	THICKNESS OF SHELL PLATE T_1 mm	THICKNESS OF DECK PLATE T_2 mm
T-1	1.6	1.2
T-2	2.3	3.2
L-1	1.6	1.2
L-2	2.3	3.2
L-3	2.3	2.3
L-4	3.2	3.2

Fig. 2 Stem models

2.3 Testing Equipment and Measurement Method

The support jigs of the side model were fixed on the table of a

Table 1 Comparison between Actual Ships and Stem Models

Structural dimensions \ Stem	Actual Ship			Models			
	Ship A*	Ship B*	Fuji**	T-1 L-1	T-2 L-2	L-3	L-4
Stem shell plate thickness mm	21	25.4	45	1.6	2.3	2.3	3.2
Stem deck plate thickness mm	10	10	23	1.2	3.2	2.3	3.2
Breast hook plate thickness mm	15	11	—	1.2	1.2	1.2	1.2
Frame spacing mm	800	400	400	50	50	50	50
Moment of inertia per unit breadth cm^3	1880	165	—	0.04	0.04	0.04	0.04
Cross-sectional area per unit breadth cm^2	3.08	3.51	—	0.24	0.24	0.24	0.24

* Reference material NSR-3-Kan 2. Outline of Strength Tests on Collision Resistance Structures

** Technical Bulletin of Nippon Kokan K.K. No. 34, 1965
New Antarctic Observation Ship "Fuji", Part 1.

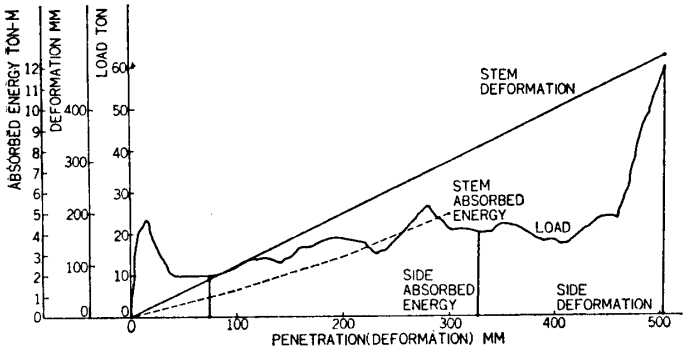

Fig. 3 Relation between load, deformation, absorbed energy and penetration of stem model T-1.

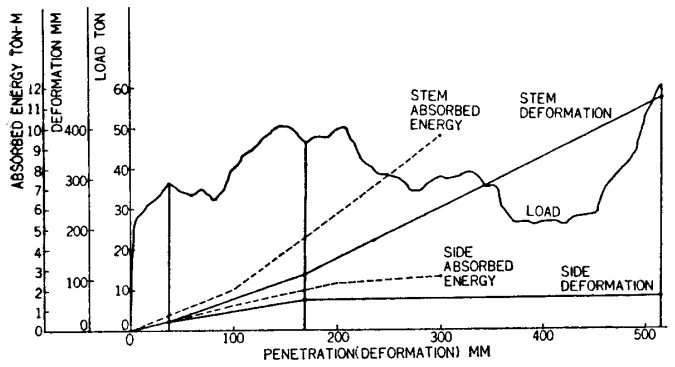

Fig. 4 Relation between load, deformation, absorbed energy and penetration of stem model L-1.

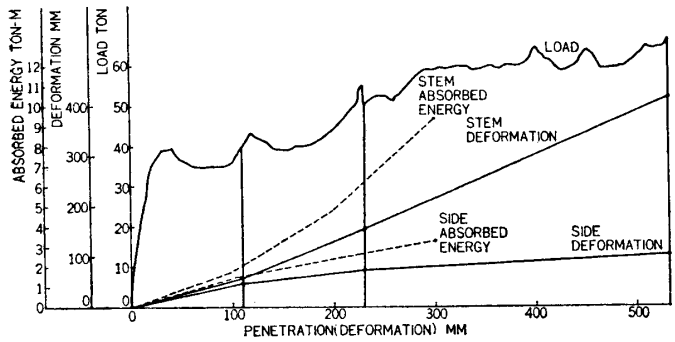

Fig. 5 Relation between load, deformation, absorbed energy and penetration of stem model T-2.

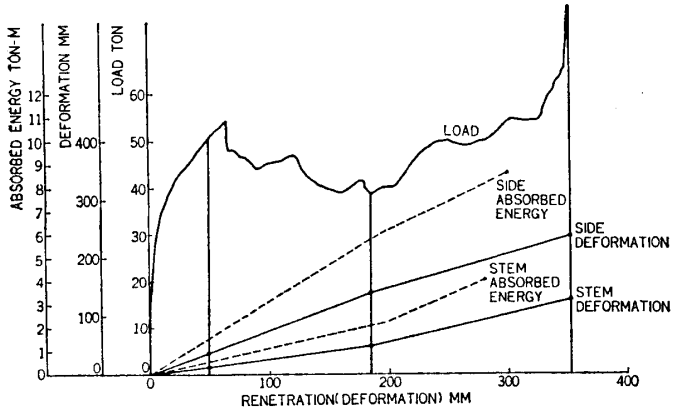

Fig. 6 Relation between load, deformation, absorbed energy and penetration of stem model L-2.

600 ton Amsler universal testing machine, and the edges of the side shells and three decks of the model were respectively welded to the support jigs through thick plates, so as to make the edge fixed. Further, the stem model was fixed on the upper part of the testing machine. The penetration tests were conducted at the loading speed of about 3 ton/minute, making the loading speed as slow as possible to avoid the effects of loading speed. The measurement items are load, penetration, deformation, stress, and destruction.

3 Test Results and Discussions

As the test results of 6 models, their load-penetration curves, measured deformation values at the middle portion of each model for both stem and side models and calculated absorbed energy are shown in Figs. 3~8. The sum of deformation values for both stem and side models is equal to the penetration.

3.1 Destruction Modes

Six load-penetration curves are collectively shown in Fig. 9. As for the destruction modes, they can be grouped into 3 types: weak stem, medium-strength stem, and strong stem.

3.1.1 Weak Stem (T-1)

In this case, panel buckling starts at the shell portion of the stem tip surrounded by decks and the first transverse frame. Thereby a part of the panel loses load bearing capacity, and the load increases until the stress of effective width of the panel portion reaches yield stress. As for the maximum load, the experimental value of 23.2 ton agrees with the calculated value* of 24 ton. This may show that the stress is nearly uniform in the shell panel of the

* Concern the calculation of buckling values. The calculated results are shown in Table 2 and the formula for calculation is explained in the appendix.

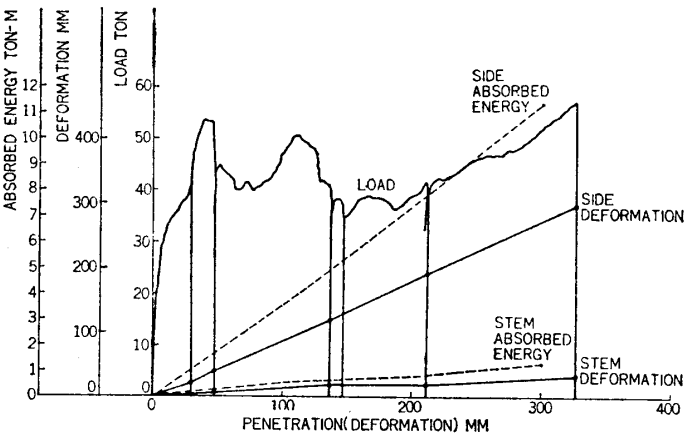

Fig. 7 Relation between load, deformation, absorbed energy and penetration of stem model L-3.

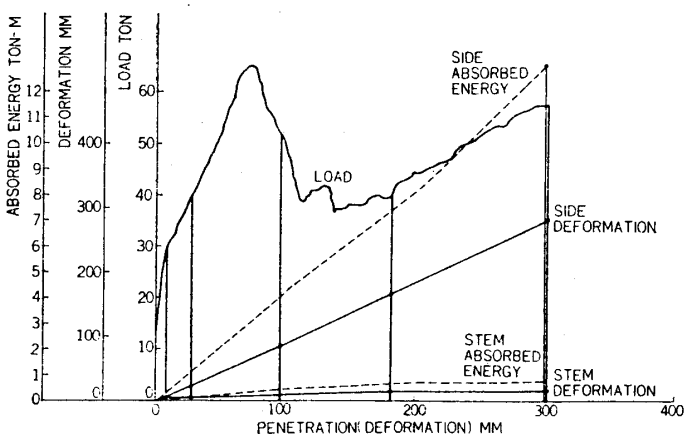

Fig. 8 Relation between load, deformation, absorbed energy and penetration of stem model L-4.

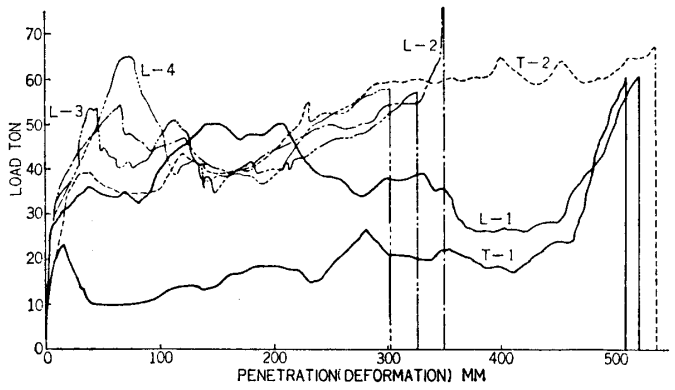

Fig. 9 Comparison of relations between load and penetration of stem models

stem tip portion and the stresses shifting in the decks are small.

The panel buckling values in the second region between 1st and 2nd frames are calculated to be of about the same value, while they are low compared with those in the first region according to the tests. It is considered that affected by buckling in the first panel at the stem the second panel has already been deformed, and its load bearing capacity has decreased. Thereafter shell panels between transverse frames will be buckled one after another under loads of similar magnitude. The gradual load increase with the increase of penetration is considered due to the increase of the load bearing area in the decks which are buckled concurrently with the shell.

Since the side model is stronger than the stem one, deformation on the side one is zero.

3.1.2 Medium-Strength Stem (T-2 and L-1)

Stem models having medium-strength are T-2 and L-1, however the destruction modes of the two are considerably different.

T-2. In the initial stage, panel buckling starts at the shell portion similar to T-1. Since the experimental value of maximum load is 39.2 ton and about twice that of T-1, the side model receives a considerable dent damage, and a small crack occurs on the side shell at the location in contact with the stem deck. Thus, the penetration, which is the sum of the stem and side deformations, is larger than that of T-1. As shown in Table 2, the calculated value of maximum load is 43.9 ton and the test value is some what lower. This is considered to be caused by the load applied to the stem, which is not only in-plane load along the stem shell but also lateral load through contact surfaces of the side model, due to large deformations in side model.

The load drops from the maximum, and then the buckling in the second region starts. However, unlike T-1, since the stem decks are strong, deck deformations are small, and the stem decks start to rupture the side shell and cut into it in a saw tooth pattern. Gradual load increase is due to the increase of the load bearing area in the decks, similar to T-1. Since the load is large, the side shell is ruptured at the location in contact with the stem decks. It is found that even though the stem

Table 2 Comparison between Calculated and Test Values for Stem Buckling Load

Name of Tests	Calculated				Test	Remark
	Stress, kg/mm²			Load, ton	Load, ton	
	Panel Buckling σ_{EP}	Maximum σ_M	Total Buckling σ_{EB}	Maximum	Maximum	
T-1	5.7	14.4	22.2	24.0	23.2	Test value is stem buckling load
T-2	11.7	18.4	21.4	43.9	39.2	
L-1	76.0	—	14.9	35.5	36.4	Test value is side shell rupture load
L-2	162.0	—	16.0	49.3	54.2	
L-3	162.0	—	16.0	49.3	53.5	
L-4	312.0	—	18.3	72.8	65.0	

The yield point of material is taken at $\sigma_y=23$ kg/mm² from the result of material tests. Calculated values are obtained by modeling the shell portion of a transversely framed stem and a longitudinally framed stem as shown in the appendix.

model is of the transversely framed type with this degree of the rigidity of the stem deck, the side shell is ruptured.

L-1. As the panel buckling values of the shell portion surrounded by longitudinal frames are considerably high, buckling occurs in the shell plate, which has the longitudinal frames as stiffeners. Against the experimental value of 36.4 ton for the buckling load, the calculated value is 35.5 ton as shown in Table 2. The calculated value is obtained by assuming a rectangular plate subjected to uniform compressive stress and the stem length measured along the shell as the buckling length. The actual conditions of the stem shell are such that stress is high at the stem tip portion and becomes less as distant from the tip, and a fair percentage of the force flows towards the decks, which is known from the results of strain measurements. Therefore the buckling mode does not encompass the full span of the stiffened plate and about a 1/3 portion of the stem shell is buckled and folded. The remaining shell portions do not deform. In considering these factors, the buckling load should be somewhat higher calculated.

The buckling in the second region occurs along 1/3 of the total span in the middle portion with the load higher than that of the first region. It is considered that the effects of the shell's bending deformations are small, on the other hand, the load bearing area of the decks has increased, and the buckling length is smaller than that of the first region. Because of high buckling load, the side shell which has already received dent damage is partly ruptured.

Although the stem decks are of the longitudinally framed type, they are buckled and folded as in T-1 since plate thickness is small. But the process is considerably different from T-1. As a whole, this case is close to the case of T-2, since a part of the side shell is ruptured.

3.1.3 Strong Stem (L-2, L-3 and L-4)

The test values of maximum loads, 54.2 ton, 53.5 ton and 65.0 ton for L-2, L-3 and L-4 respectively are the rupture loads of the shell in side models. The destruction of 3 stem models under those loads are dent damages (partial buckling) on the stem tip portion, and small cracks at the location in contact with the side decks. The stem buckling loads of 49.3 ton, 49.3 ton and 72.8 ton are calculated by considering a rectangular plate subjected to uniform compressive stress as in L-1. In consideration of actual stress distribution and buckling wave, stem buckling load should be higher calculated.

Difference in the number of maximum load peaks depends upon two rupture modes of the side shell by the stem: (1) along its full breadth or (2) along its half breadth. However, this is considered due to nonuniform load application and does not represent the basic differences.

After the side shell is ruptured, the load decreases, and while the stem shell and side decks are tearing each other, penetration increases. Although plate thickness of the stem shell of 2.3 mm for L-2 and L-3 and of 3.2 mm for L-4, is equal to or smaller than that of the side deck of 3.2 mm, the area of tearing in the stem shell is smaller. This is considered due to the fact that even though the stem shell is supported at both ends by the stem decks, the restraint is weak. On the other hand, side decks are fixed at both ends by rigid jigs, and the restraint is strong and high tensile stress is induced in the side decks.

L-2 and L-3 have different plate thickness of stem deck, however, actual tests reveal no differences. It is considered that if the rigidity of the stem decks is above a certain level the buckling and folding of the stem is prevented, and there would not be any other effects of the plate thickness.

3.2 Absorbed Energy at Destruction

The energy absorbed by the destruction of structure can be calculated by the product of load and deformation that the structure undergoes. In Figs. 3～8, deformation and absorbed energy of the respective stem and side structures are also shown.

3.2.1 Relation between Absorbed Energy at Destruction and Stem-Side Strength Ratio

Comparisons between absorbed energy of both stem and side obtained by tests, are shown in Fig. 10. The structural strength ratio of stem to side is taken as abscissa. For the strength of the stem, the calculated maximum load, namely the smaller of the calculated buckling load shown in Table 2 or yielding load is used, and for the strength of the side, 58 ton is used which is the result of the experiment in case of the rigid stem. Penetration is taken as parameters. From this figure, it can be noted that the destruction mode changes at the strength ratio of about 0.8. Below or above this point either the stem or the side is destructed one-sidedly.

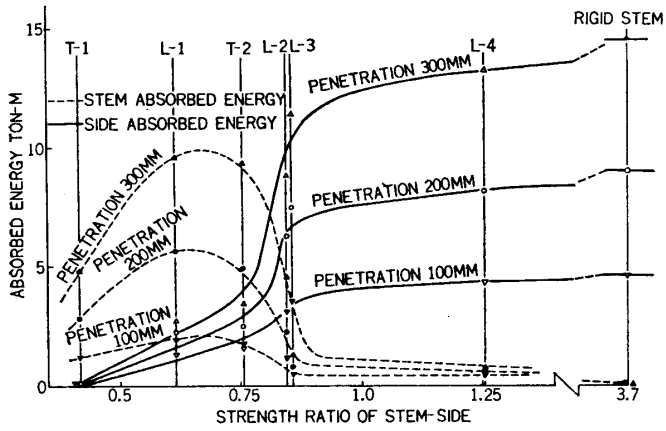

Fig. 10 Relation between strength ratio of stem to side and absorbed energy

As discussed in 3.1., the values of the maximum load for longitudinally framed type L-1～4 are calculated on the assumption that compressive stress is uniformly distributed, and the actual maximum loads are somewhat higher than calculated values. When the value of this extra load is so chosen that the strength ratio at changes in destruction mode becomes 1.0, correction factor becomes 1.0/0.8=1.25. By using this factor the strength ratios of longitudinally framed structures are

L-1: 0.76, L-2 and L-3: 1.06, L-4: 1.56.

Then, they should be interpreted by shifting their positions along the abscissa.

3.2.2 Comparison between Conversion Values into Actual Ships and Calculated Values by Minorsky's Method

In considering the fact that test models are reduced to a scale of 1/10 of actual ships, the conversion values into actual ships may be estimated as follows:

$$\text{load} \times 10^2,\ \text{penetration} \times 10^1,\ \text{absorbed energy} \times 10^3.$$

Conversion values of absorbed energy into actual ships and calculated values by Minorsky's method are shown in Table 3. Minorsky's equation is expressed as follows:[1)]

$$\text{K.E.} = 175.8\ R_t + 124{,}000 \qquad (1)$$

$$R_t=1.33\,\Sigma\ P_aL_at_a+\Sigma\ P_bL_bt_b+\Sigma\ 1.4\,P_a\times 1.5\,\mathrm{m}\times t_s \qquad (2)$$

where K.E.: absorbed energy (ton-kt²), R_t: resistance coefficient (m²—mm), P: depth of penetration (m), L: width of penetration (m), t: plate thickness (mm), Subscripts a,b,s: deck of ship subjected to collision, deck in the stem of the colliding ship, shell in the stem of the colliding ship.

Table 3 Conversion Values of Absorbed Energy into Actual Ship*,**

Name of Tests	Penetration m	Side Absorbed Energy		Stem Absorbed Energy		Total Absorbed Energy	
		Test Values	Calculated Values	Test Values	Calculated Values	Test Values	Calculated Values
T-1	1	0	0.7	1.3	0.7	1.3	4.9
L-1		0.9		2.0		2.9	
T-2		1.4		1.8	1.2	3.2	5.4
L-2		3.1		1.1		4.2	
L-3		3.5		0.6	1.1	4.1	5.3
L-4		4.3		0.5	1.5	4.8	5.7
T-1	2	0	2.9	2.8	1.8	2.8	8.2
L-1		2.3		5.6		7.9	
T-2		2.4		4.8	3.6	7.2	10.0
L-2		6.2		2.3		8.5	
L-3		7.4		0.8	3.0	8.2	9.4
L-4		8.1		0.7	4.1	8.8	10.5
T-1	3	0	6.4	4.9	3.3	4.9	13.2
L-1		2.6		9.6		12.2	
T-2		3.3		9.4	6.9	12.7	16.8
L-2		8.7		4.5		13.2	
L-3		11.4		1.3	5.6	12.7	15.5
L-4		13.2		0.8	7.8	14.0	17.7

* Side absorbed enegy $=1.33\,\Sigma\ P_aL_at_a\times 175.8\times 0.027$

** Stem absorbed energy $=(\Sigma\ P_bL_bt_b+\Sigma\ 1.4\,P_a\times 1.5\,\mathrm{m}\times t_s)\times 175.8\times 0.027$

Total absorbed energy = Side and stem absorbed energy + 124,000 × 0.027

Unit of absorbed energy $=\times 10^3$ ton-m

Calculated values are according to equations (1) and (2) by Minorsky's method

Absorbed energy corresponding to each penetration is calculated from the above equation, where it is taken that 1 ton-kt²=0.027 ton-m. From Table 3 it is clear that, while estimated values of absorbed energy by Minorsky's method differ considerably from test values when compared individually for the stem and the side, the total values including the constant 124,000 ton-kt² in the case of calculated values agree with test values as a whole. In a weak stem (T-1), since actually only the stem breaks, Minorsky's method, which assumes breaking of both the stem and side, tends to overestimate the absorbed energy of the side. In medium-strength stem (L-1, T-2) and a strong stem (L-2), since both the stem and side destruct, and this actually agrees with Minorsky's assumption, the estimated values of absorbed energy for the stem, side and total agree with the test values for the total range of penetration (1~3 m). In a very strong stem (L-3, L-4), it is noted that Minorsky's method tends to underestimate the absorbed energy of the side, and overestimate that of the stem.

4 Examination of Design Formula

Design formula is investigated from the test results. By summarizing the test results Figs. 11~12 are obtained. Fig. 11 shows the relation between absorbed energy ratio f and strength ratio of stem to side λ. Penetration w at the time of test is used as the parameter.

Here
$$f=\frac{E}{E_s},\qquad \lambda=\frac{P_B}{P_A},\qquad E=E_A+E_B,\quad w=w_A+w_B \qquad (3)$$

where f: ratio of the total absorbed energy in case of an elastic stem to absorbed energy in case of a rigid stem, λ: strength ratio of stem to side, E: total absorbed energy of the collided ship and colliding ship, E_A: absorbed energy of the side of a collided ship, E_B: absorbed energy of the

stem of a colliding ship, E_s : absorbed energy of a collided ship due to a rigid stem, P_A : rupture load of the side of a collided ship, P_B : buckling load of the stem of a colliding ship, w : penetration (relative displacement), w_A : dent in the side of a collided ship, w_B: crush of the stem of a colliding ship.

Fig. 12 shows the absorbed energy ratio of side to total γ and the penetration ratio of side to total δ.

Here, $$\gamma=\frac{E_A}{E}, \qquad \delta=\frac{w_A}{w}. \quad (4)$$

From the test results of Fig. 11, an experimental formula is obtained in the form,

$$f(\lambda)=\begin{cases}0 & :\lambda<0.4\\ (\lambda-0.4)^{0.25} & :0.4\leq\lambda\leq1.4\\ 1 & :1.4<\lambda\end{cases} \quad (5)$$

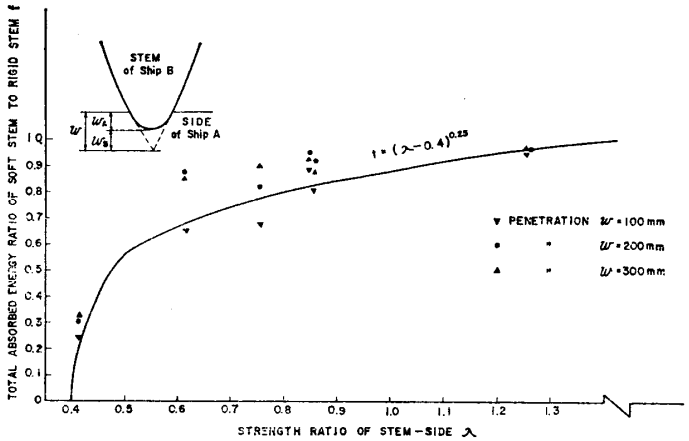

Fig. 11 Relation between strength ratio and total absorbed energy ratio

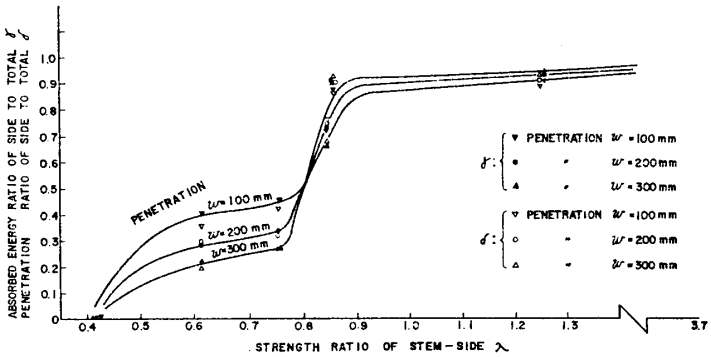

Fig. 12 Relation between strength ratio, absorbed energy ratio and penetration ratio

According to Fig. 12, it is shown that for $\lambda\lesssim0.8$, γ and $\delta\lesssim0.5$, and also for $\lambda<0.8$, as the penetration increases, γ, δ decreases while for $\lambda>0.8$ its reverse holds true. Namely, strength ratio of stem to side being 0.8 as a border, it can be seen that the destruction on a weaker structure is greater, and that as penetration increases the rate of destruction on a weaker structure increases. For the case of a general elastic stem which penetrates into the side of a nuclear powered ship, the total absorbed energy of both stem and side can be expressed in the form.

$$E=f(\lambda)E_s(w) \quad (6)$$

The relation between the absorbed energy and penetration by rigid stem can be expressed by eq. (7) when the side deck is stronger than the side shell[5].

$$E_s(w)=Nt_d\sigma_0\tan\theta w^2 \quad (7)$$

where N : number of deck layers, t_d : deck plate thickness, σ_0 : material constant (use 80% of yield point), θ : a half of stem angle, w : sum of penetrations for both stem and side. In case of penetration of a rigid stem, penetration of side only.

From eqs. (6) and (7), the relation between the absorbed energy and penetration by an elastic stem can be expressed by eq. (8),

$$E=\beta(\lambda)Nt_d\sigma_0\tan\theta w_A^2 \quad (8)$$

where $\beta(\lambda)$: $f(\lambda)/\delta^2$, correction factor relative to absorbed energy by a rigid stem.

Now, the strength ratio of stem to side λ as well as the penetration ratio δ and the correction factor of absorbed energy β are obtained by using a buckling load for the stem and a rupture load for the side, which has been obtained either as experimental or calculated values. While in above-mentioned tests the ship side is assumed to be nearly the same as that of Mutsu, it would be necessary to consider the cases of sides of other nuclear powered ships also. Here, as side models, Mutsu and the Savannah of U.S.A., while as stem models, the T-2 tanker (as representative of the general

Table 4 Strength ratio, absorbed energy ratio, penetration ratio and correction factor between side and stem structures

Side Model	Stem Model	λ	f	δ	β
Mutsu	T-2 Tanker	0.57	0.64	0.30	7.1
	Ship B	1.01	0.88	0.90	1.1
	Fuji	1.86	1.00	1.00	1.0
Savannah	T-2 Tanker	0.77	0.78	0.45	3.8
	Ship B	1.37	0.99	0.95	1.1
	Fuji	2.51	1.00	1.00	1.0

λ : strength ratio of stem to side
f: total absorbed energy ratio of soft stem to rigid stem
δ : penetration ratio of side to total
β : correction factor for total absorbed energy
breaking load of side structure
Mutsu=58 ton
Savannah=43 ton
buckling load of stem T-2 Tanker=33 ton
Ship B=59 ton
Fuji=108 ton

sum of ships), ship B (ice-strengthened ship) and "Fuji" (icebreaker) are considered. They are shown in Table 1, and the strength ratio of stem to side, etc. for these ships are calculated and shown in Table 4. Both stem and side are assumed as approximately 1/10 scale model. As the buckling load of the stem and the rupture load of the side, experimental values are used for Mutsu and calculated values are used for other ships. From Table 4, it is noted that in case of the collision between Mutsu and T-2 tanker, since T-2's stem is of the elastic type, hence absorbed energy due to destruction of the stem would be large. In this case both stem and side can absorb the amount of energy equivalent to approximately 7 times (β=7.1) that of the side when assumed to be collided by a rigid stem. On the other hand in the collision case between Savannah and T-2 tanker, since the strength of the side of Savannah approaches that of stem of T-2 tanker, consequently the absorbed energy of the stem becomes ess. It can be considered that as Mutsu is of small size in comparison with Savannah, its side structure was designed with relatively greater strength. That β value of Mutsu is about two times larger than that of Savannah indicates that two times larger energy can be absorbed in Mutsu at the same penetration when collided by an elastic stem. In the future if the size of the nuclear powered ship increases, and ships larger than Savannah become standard, the assumption that correction factor β is unity will make the design of the side structure in the safety side.

Now, in designing the side structure of nuclear powered ships, once the nuclear reactor space and its distance from the side shell w_d is established, eq. (9) will become one of design specifications so that side penetration will not exceed it in the time of collision:

$$w_A \leq w_d \ . \tag{9}$$

When one ship is collided by another ship, of the total kinetic energy of the colliding ship, the share which must be absorbed by the side of collided ship is in the form,

$$E_k = \frac{M_B}{2} \cdot \frac{M_A + d_m}{M_A + d_m + M_B} (V_B \sin\phi)^2 \tag{10}$$

where E_k : kinetic energy to be absorbed, M_A : mass of collided ship (nuclear powered ship), M_B: mass of colliding ship, V_B : speed of colliding ship, ϕ : colliding angle, d_m : added mass of water.

By using eqs. (10) for the energy to be absorbed by the side, (8) for the energy that can be absorbed and (9), the following formulae are obtained:

$$Nt_d \geq \frac{M_B}{2} \frac{M_A + d_m}{M_A + d_m + M_B} \frac{(V_B \sin\phi)^2}{\beta(\lambda)\sigma_0 \tan\theta\, w_d^2}, \quad V_B^2 \leq \frac{2}{M_B} \frac{M_A + d_m + M_B}{M_A + d_m} \frac{\beta(\lambda) Nt_d \sigma_0 \tan\theta\, w_d^2}{\sin^2\phi}. \tag{11}$$

5 Conclusion

In a collision between a nuclear powered ship and a conventional ship or a ship having higher rigidity such as ice-strengthened ship or icebreaker, in order to investigate the share of absorbed energy according to the strength ratio of the stem of the colliding ship to the side structure of a nuclear powered ship, six collision tests were conducted between the side structure simulating Mutsu

and elastic stems simulating conventional ships and more rigid ships.

Conclusions obtained are as follows:

(1) Destruction modes of the stem and the side structures can be grouped according to the strength of stems :

a. weak stem, b. medium-strength stem, c. strong stem.

a. corresponds to conventional ships having transversely framed stem, and buckling occurs unilaterally on the stem.

b. corresponds to icebreakers of the transversely framed type or conventional ships having longitudinal frames, and the stem penetrates into the side shell with buckling, and sometimes ruptures the side shell.

c. corresponds to icebreakers having longitudinal frames, and the side shell is usually ruptured, while the stem is not buckled, though sometimes ruptured to some degree by the side decks.

(2) Since Minorsky's calculation method for estimating the absorbed energy is based on the assumption that both stem and side destruct at the time of collision, it is considered appropriate for the case of (1) b. But for (1) a. and c., it overestimates the absorbed energy of the stronger structures, because they are actually not destructed extensively.

(3) From the result of collision tests, the relation between absorbed energy and penetration for an elastic stem and design formula for the collision-protective structures of nuclear powered ships is obtained. In case of collision by an elastic stem, a considerable quantity of energy is expected to be absorbed by the stem, hence the design formula based on the collision tests by a rigid stem will give structural dimensions fairly in the safety side.

Acknowledgement

This study was taken charge of by authors as a part of the work of the Nuclear Ship Research No. 3 Committee of Japan Shipbuilding Research Association (chairman Yoshio Akita) and examined in the committee. Acknowledgement is due to Dr. N. Ando of Ship Research Institute of Japan, Prof. Y. Fujita of University of Tokyo and other members of the Committee who discussed the results of experiments and collaborated in preparing this paper. The paper is presented by permission of the Association, but responsibility for statements or opinions rest with the authors.

References

1) Minorsky, V. U., "An analysis of ship collision with reference to protection of nuclear power plants", *Journal of Ship Research*, Jg. 3, H. 2, (1959).

2) Akita, Y., Takada, K., Ushioda, S., Matsuzawa, S., Kataoka, G., "The report of the collision barrier of nuclear powered ship", *Journal of the Society of Naval Architects of Japan*, Vol. 118 (1965), (in Japanese).

3) Spinelli, F., "La sicurezza del reattore nucleare a bordo delle navi mercantili, *Tecnica Italiana*, Anno XXVIII-N. 12 (1963).

4) Woisin, G., "Kollisionsversuche mit Schiffsteilmodellen, *Kerntechnik*, 9 (1967).

5) Third Nuclear Shipbuilding Research Committee, "Studies on Collision and Explosion Protective Structure of Nuclear Powered Ship", *Japan Shipbuilding Research Association, Research Bulletin*, No. 122, March, (1970).

6) Yamamoto, Y., "Elasticity and plasticity", *The Lecture of Applied Mathematics and Dynamics*, No. 11 Asakura Shoten, (1961), (in Japanese).

Appendix

Calculation of buckling load for stem models.

Since the stem shell has transverse or longitudinal stiffeners, the buckling of a stiffened plate is considred[6]. Two kinds of bucklings occurring in stiffened plates are

(1) buckling of a panel surrounded by stiffeners, σ_{EP}, and

(2) total buckling of a stiffened plate, σ_{EB}.

Local buckling of a stiffener is omitted to consider because it does not occur in stem models.

$$\sigma_{EP}=\min_{m}\frac{\pi^2 D}{tb^2}\left(\frac{mb}{a}+\frac{a}{mb}\right)^2 \tag{A.1}$$

$$\sigma_{EB}=\min_{m}\frac{\pi^2}{(t+A_x/b_x)b^2}\left\{D_x\left(\frac{mb}{a}\right)^2+2H+D_y\left(\frac{a}{mb}\right)^2\right\} \tag{A.2}$$

where, a,b: longitudinal and transverse lengths of a rectangular plate, a are 90 sec 30°mm and 600 sec 30°mm for the stems with transverse frams and those with longitudinal frams respectively, and b is 300 mm for both stems. t : plate thickness, A_x : sectional area of stiffeners, b_x : stiffener space, D, D_x, D_y : bending rigidities of a plate and a stiffened plate along x and y axis, H : torsional rigidity of a stiffened plate, subscripts x, y : direction parallel and perpendicular to stiffeners.

In case of $\sigma_{EP}<\sigma_{EB}$, panel buckling occurs but load increases until the stress of the effective width of a panel reaches yield stress. Maximum stress of a stiffened plate is expressed using Marguerre's formula,

$$\sigma_M=\sqrt[3]{\sigma_{EP}\sigma_y^2} \tag{A.3}$$

where σ_y : yield stress. In case of $\sigma_{EB}<\sigma_{EP}$, total buckling occurs and a stiffened plate cannot support any more load.

Buckling stresses and maximum loads for stem models T-1～2 and L-1～4 were calculated and shown in Table 2.

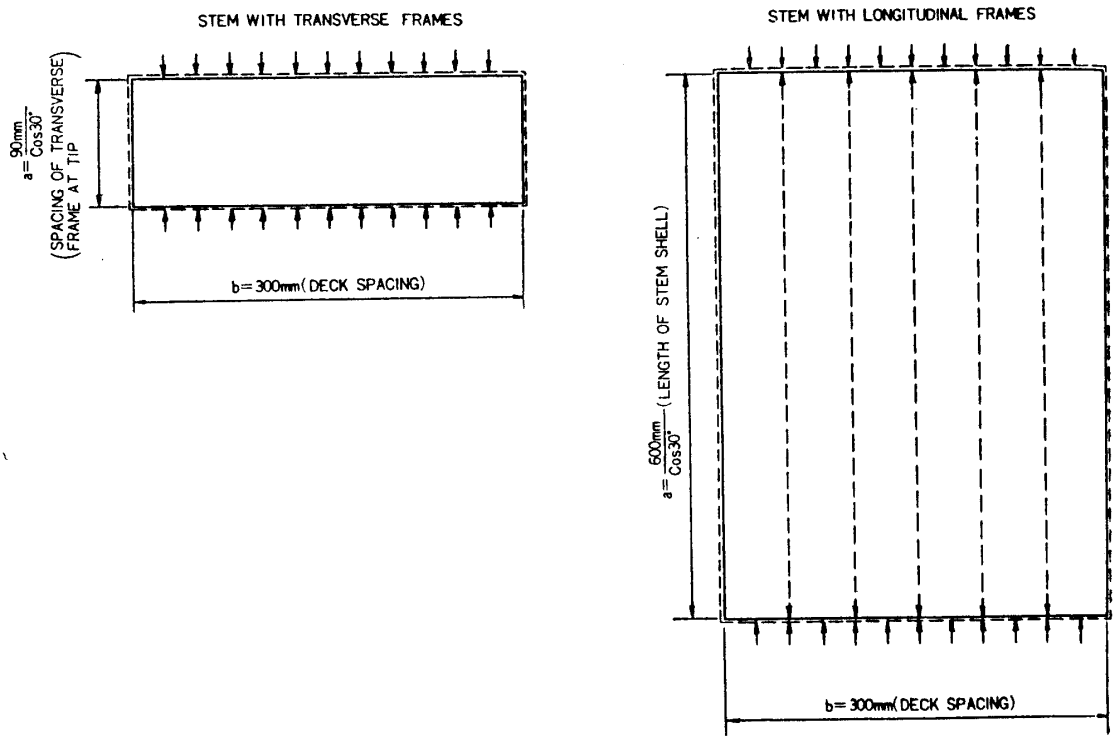

Fig. A 1 Models of the shell portion of a transversely framed stem and a longitudinally framed stem